

Published in final edited form as:

*DNA Repair (Amst)*. 2006 February 3; 5(2): 243–250. doi:10.1016/j.dnarep.2005.10.005.

## BCR/ABL modifies the kinetics and fidelity of DNA double-strand breaks repair in hematopoietic cells

Artur Slupianek<sup>1,†</sup>, Michal O. Nowicki<sup>1,2,†</sup>, Mateusz Koptyra<sup>1</sup>, and Tomasz Skorski<sup>1,\*</sup>

<sup>1</sup>Center for Biotechnology, College of Science and Technology, Temple University, Philadelphia, Pennsylvania 19122

### Abstract

The oncogenic BCR/ABL tyrosine kinase facilitates the repair of DNA double-strand breaks (DSBs). We find that after  $\gamma$ -irradiation BCR/ABL-positive leukemia cells accumulate more DSBs in comparison to normal cells. These lesions are efficiently repaired in a time-dependent fashion by BCR/ABL-stimulated non-homologous end-joining (NHEJ) followed by homologous recombination repair (HRR) mechanisms. However, mutations and large deletions were detected in HRR and NHEJ products, respectively, in BCR/ABL-positive leukemia cells. We propose that unfaithful repair of DSBs may contribute to genomic instability in the Philadelphia chromosome-positive leukemias.

### INTRODUCTION

The *bcr/abl* chimeric gene is derived from fusion of part of the *c-abl* gene from chromosome 9 to part of the *bcr* gene locus on chromosome 22 [t(9;22), Philadelphia chromosome=Ph<sup>1</sup>], and is present in most chronic myelogenous leukemia (CML) and a cohort of acute lymphocytic leukemia (ALL) patients [1,2]. BCR/ABL exhibits two complementary roles in cancer: stimulation of signaling pathways that render leukemia cells independent of their environment and modulation of the response to DNA damage causing drug resistance [3,4]. In contrast to normal cells, BCR/ABL-positive cells seem to be better equipped to survive genotoxic damage due to their enhanced ability to repair DNA lesions, prolonged activation of the G2/M checkpoint to provide more time for repair, and inhibited pro-apoptotic mechanisms [5]. Clinical observations and experimental findings have shown that BCR/ABL stimulates also genomic instability, leading to mutations and chromosomal abnormalities [6-12]. The accumulation of genetic errors is believed to be responsible for the transition from a relatively benign CML chronic phase (CML-CP) to the aggressive blast crisis phase (CML-BC) [13]. Aberrations in pathways regulating the DNA damage response in BCR/ABL-positive leukemia cells may contribute to this phenomenon.

DNA damage can directly result from genotoxic treatment and genotoxic effects of compounds such as reactive oxygen species (ROS). Recently we showed that BCR/ABL-

© 2005 Elsevier B.V. All rights reserved.

\* Correspondence: Tomasz Skorski, Center for Biotechnology, College of Science and Technology, Temple University, Bio-Life Sciences Building, Room 419, 1900 N. 12<sup>th</sup> Street, Philadelphia, PA 19122, tskorski@temple.edu

† A.S. and M.O.N. contributed equally to this work.

<sup>2</sup> Present affiliation: Department of Neurological Surgery, The Ohio State University Medical Center, Columbus, OH 43210

**Publisher's Disclaimer:** This is a PDF file of an unedited manuscript that has been accepted for publication. As a service to our customers we are providing this early version of the manuscript. The manuscript will undergo copyediting, typesetting, and review of the resulting proof before it is published in its final citable form. Please note that during the production process errors may be discovered which could affect the content, and all legal disclaimers that apply to the journal pertain.

positive leukemia cells contain elevated levels of DNA double-strand breaks (DSBs) induced by ROS, whose unfaithful repair may contribute to genomic instability [14]. Unfaithful repair of the “spontaneous” DSBs in CML cells was also reported by others [15]. Since BCR/ABL-positive cells are resistant to genotoxic treatment [4], survivors may harbor errors leading to genetic instability and malignant progression of the disease. This hypothesis was tested here.

This work shows that BCR/ABL-positive leukemia cells accumulate more DSBs than normal counterparts after  $\gamma$ -irradiation. However, the oncogene facilitates homologous and non-homologous DSBs repair mechanisms, which generate mutations and deletions. Therefore, we hypothesize that elevated levels of DSBs combined with unfaithful repair mechanisms may contribute to genomic instability and malignant progression of the Ph<sup>1</sup>-positive leukemia cells, which survive genotoxic treatment. This speculation is supported by the observation that BCR/ABL cells surviving irradiation may carry additional chromosomal aberrations [11].

## METHODS

### Cells

The murine growth factor-dependent myeloid cell line 32Dcl3 and BCR/ABL-expressing clones were described previously [16]. 32Dcl3 cells were electroporated with the expression plasmid containing DR-GFP recombination substrate and *pgk-pur* gene [17]. Puromycin-resistant clones were selected and genomic integration of DR-GFP cassette was detected by Southern blotting. A clone containing a single copy of DR-GFP was electroporated with pSR $\alpha$ -p210BCR/ABL-neo or pSR $\alpha$ -neo retroviral construct, and cells were selected in G418. Three DR-GFP clones expressing BCR/ABL (confirmed by Western analysis) or displaying resistance to G418 (control) were selected and used for the experiments. Cells were maintained in the presence of pre-tested optimal concentrations of IL-3 required to maintain continuous proliferation of parental cells. In these conditions parental and BCR/ABL-transformed cells displayed similar cell cycle profile.

### Western analysis

To prepare whole cell lysates proteins were solubilized in cold NP-40 lysis buffer (10mM HEPES, pH 7.5, 150mM NaCl, 1% NP-40, 10% glycerol) with protease inhibitors (1mM dithiothreitol, 1mM phenylmethylsulfonyl fluoride, 50mM NaF, 1mM Na<sub>3</sub>VO<sub>4</sub>, 10  $\mu$ g/ml aprotinin and 10  $\mu$ g/ml leupeptin) and 10  $\mu$ g/ml RQ1 DNase (Promega, Madison, WI). Protein samples were separated by SDS-PAGE and analyzed by Western blotting using the following antibodies: anti-Ku70 and anti-Ku80 (both rabbit polyclonal from Serotec, Raleigh, NC); mouse monoclonal anti-RAD51 (Upstate USA, Charlottesville, VA); mouse monoclonal anti-actin (Calbiochem, San Diego, CA).

### Examination of HRR efficiency and fidelity

HRR events were measured as described before [16,18] with modification. Cells were electroporated with 100 $\mu$ g of pC $\beta$ A-Sce expression plasmid encoding I-SceI endonuclease and 20 $\mu$ g of pDsRed1-Mito (Clontech, Palo Alto, CA). Expression of I-SceI causes a DSB in the specific restriction site included in the DR-GFP cassette, and pDsRed1-Mito encodes red fluorescent protein with a mitochondrial localization signal to control the efficiency of transfection. HRR event restores functional GFP expression, which is readily detected by fluorescent microscope 48h after transfection with I-SceI. HRR efficiency was established as percentage of cells displaying green nuclear fluorescence and red mitochondrial fluorescence versus all transfected (red) cells. The efficiency of transfection was 36% and 35% in 32Dcl3 and BCR/ABL-expressing clones, respectively, containing DR-GFP reporter

cassette. GFP<sup>+</sup> cells were sorted and a fragment of the DR-GFP cassette containing a DSB repair site was amplified by PCR and sequenced as described [14]. HRR mutation frequency was calculated as: total number of mutated nucleotides/total number of sequenced nucleotides (20 sequences/group analyzed).

### Examination of NHEJ efficiency and fidelity

NHEJ was measured in cell-free extracts as described before [14]. When indicated cell lysates were deprived of Ku70 and Ku80 by incubation with agarose beads pre-coated with anti-Ku70 and anti-Ku80 antibodies or with non-immune isotype-matched immunoglobulins (confirmed by Western analysis). The substrates were pBluescript KS<sup>+</sup> linear plasmids digested XhoI+XbaI or SmaI to generate non-compatible 5' overhangs or blunt-ends, respectively. NHEJ products were amplified by PCR using the following primers: 5' primer: TGCGCAACTGTTGGGAAG, 3' primer: TGTGGAATTGTGAGCGGATA. Amplification products were cloned into the pETBlue Acceptor Vector Kit (Novagen) and sequenced using 5' primer: ATTTCCATTCGCCATTCAG. An average gain/loss of the bases in the NHEJ sequences was determined by dividing the sum of acquired/deleted bases by the number of sequences. Twenty NHEJ products/experimental group were analyzed.

### Immunofluorescence

Cells were irradiated with the indicated doses from <sup>137</sup>Cs source. Nuclear localization and co-localization of the indicated proteins was detected by immunofluorescence as previously described [14]. Briefly, cytopins were fixed and stained with primary antibodies against  $\gamma$ -H2AX (Upstate Biotechnology, Lake Placid, NY, USA) and RAD51 (PC130, Oncogene Research Products, Cambridge, MA, USA), or Ku70 (AHP318, Serotec, Inc., Raleigh, NC, USA). The secondary antibodies conjugated with FITC (Alexa488) or RHO (Alexa568) were applied (Molecular Probes Inc., Eugene, OR, USA). Negative controls were performed without primary antibodies. DNA was counterstained with 4',6'-diamidino-2-phenylindole (DAPI). Specific staining was visualized with an inverted Olympus IX70 fluorescence microscope equipped with a Cooke Sensicam QE camera (The Cooke Co., Auburn Hills, MI, USA). At least 50 individual cells were analyzed/experimental group, as described before [14].

## RESULTS

### BCR/ABL changes the kinetics of DSBs induced by $\gamma$ -irradiation in hematopoietic cells

32Dcl3 parental cells and their BCR/ABL-positive counterparts (3 clones/group) were irradiated with 4Gy to induce DSBs, which were detected by immunofluorescence using  $\gamma$ -H2AX foci co-localizing with DNA as markers [19-21]. DSBs were calculated here as percentage of DNA counterstained with DAPI co-stained with  $\gamma$ -H2AX foci. More DSBs were detected in BCR/ABL cells than parental cells before irradiation (Figure 1A-left panel) in accordance with previous report [14]. In addition, 10 min after irradiation, BCR/ABL cells displayed a sharp increase in DSBs, however, after 30min their number dropped to the levels detectable in parental cells and continued to decrease up to 12h (Figure 1A-left panel). Parental cells displayed different kinetics of DSBs induced by 4Gy; modest increase was observed during first 30min followed by a steady decrease up to 6h (Figure 1A-left panel). The increase in DSBs counts detected in BCR/ABL cells 10min after irradiation was observed also after lower doses of irradiation (Figure 1A-right panel). This effect was reduced by ~2-fold (data not shown) if BCR/ABL cells were pre-incubated for 48h with 0.2 $\mu$ M of antioxidant pyrrolidine dithiocarbamate as described before [14].

HRR and NHEJ reaction sites in the nuclei could be potentially visualized by double-immunofluorescence detecting co-localization of  $\gamma$ -H2AX foci with RAD51 or Ku70,

respectively [22,23]. Therefore, the kinetics of total cellular involvement of HRR and NHEJ in reparation of DSBs was estimated by double immunofluorescence examining the levels DNA associated with co-localizing  $\gamma$ -H2AX and RAD51 or  $\gamma$ -H2AX and Ku70, respectively (Figure 1B). As expected, NHEJ generally preceded HRR [24]. A sharp increase in total cellular  $\gamma$ -H2AX and Ku70 co-localization was detected as early as 10min after  $\gamma$ -irradiation, but BCR/ABL-positive cells displayed much higher co-localization values in comparison to parental counterparts at 10min and 30min (Figure 1B), probably reflecting much higher levels of DSBs in the former cells (Figure 1A). The amounts of total cellular  $\gamma$ -H2AX and Ku70 co-localization gradually decreased in time, and 3h after irradiation these values were indistinguishable in parental and BCR/ABL cells. A peak of total cellular  $\gamma$ -H2AX and RAD51 co-localization was observed 3h after  $\gamma$ -irradiation (Figure 1B). Again BCR/ABL cells displayed much higher levels of co-localization than parental cells at 3h and 6h after  $\gamma$ -irradiation (Figure 1B).

To assess the relative frequency of NHEJ and HRR in the repair of DSBs pool, we measured the percentage of  $\gamma$ -H2AX co-localizing with Ku70 and RAD51, respectively (Figure 1C). Parental and BCR/ABL cells displayed similar kinetics of  $\gamma$ -H2AX co-localizing with Ku70; interestingly the percentage of  $\gamma$ -H2AX co-localizing with RAD51 was higher in the latter cells especially at 3h after  $\gamma$ -irradiation.

Altogether the immunofluorescence studies implicate qualitative and quantitative changes in the kinetics of appearance and repair of DSBs in BCR/ABL cells in comparison to normal counterparts.

Western analysis revealed a sharp increase of Ku70 and Ku80 protein expression in BCR/ABL cells during first 3h after  $\gamma$ -irradiation in comparison to parental counterparts (Figure 2). In addition, BCR/ABL cells accumulated more RAD51 protein than parental cells, but this effect peaked between 3-6h after  $\gamma$ -irradiation.

### **BCR/ABL increases the efficiency, but lowers the fidelity of DSBs repair in hematopoietic cells**

pBluescript plasmid linearized by SmaI or XhoI+XbaI digestion creating blunt-ends or non-complementary 5' overhangs, respectively, was used as the substrate to assess the activity of NHEJ, which generates the products containing multimers of plasmid [25,26]. The substrate was added to cell lysates from 32Dcl3 parental and BCR/ABL cells and NHEJ products were analyzed by agarose gel electrophoresis. BCR/ABL kinase was responsible for 2-4 – fold increase of NHEJ activity (Figure 3, left panel). Deprivation of Ku70 and Ku80 from cell lysated abrogated the reaction implicating NHEJ mechanism. On average, the presence of BCR/ABL promoted loss of DNA during NHEJ (Figure 3, right panel). Typical deletions or additions (range: +14 to –49 bp) were detected in NHEJ products in parental cells. NHEJ products in BCR/ABL cells contained smaller additions and larger deletions (range: +4 to –220 bp). Interestingly, repair of blunt-ended DSB substrates (SmaI digests) generated more extensive deletions in comparison to 5' non-complementary overhangs (XhoI + XbaI digests) ( $p < 0.05$ ) implicating the potential problem with simple re-joining by ligation. Analysis of the junctions of the joints from the deletion products revealed a bias toward microhomology in NHEJ products from parental as well as BCR/ABL cells.

To obtain additional evidence that BCR/ABL stimulates HRR, a genetic model was applied, used before in non-hematopoietic cells [14]. Therefore, these studies may not reflect discrete differences in DNA repair between non-hematopoietic and hematopoietic cells. A single copy of the DR-GFP cassette containing inactivated GFP gene due to introduction of the unique I-SceI restriction site containing two stop codons and a truncated version of the gene containing BcgI restriction site was integrated into the genome of 32Dcl3 cells [17]. A DSB

is generated in the GFP gene upon transient transfection with I-*SceI* expression plasmid, which could be repaired by HRR employing the truncated fragment of the gene as a template, thus producing a functional gene containing *BcgI* restriction site and hence GFP+ cells. 32Dcl3 cells containing DR-GFP cassette were transfected with expression plasmids containing BCR/ABL or empty plasmid; the expression of BCR/ABL protein was confirmed by Western analysis (not shown). Then these cells were transfected with I-*SceI* and pDsRed1-Mito expression plasmids and the efficiency of HRR was measured 48h later by scoring the percentage of double-positive GFP+Red+ cells in all transfected cells (Red+). The presence of BCR/ABL kinase caused ~6-fold increase of the percentage of GFP+ cells implicating activation of HRR mechanism (Figure 4, HRR efficiency). The primers spanning a fragment of the DR-GFP cassette containing the DSB site were used to amplify the repair products by PCR in GFP+ cells, which were then sequenced to determine the fidelity of HRR as described before [14]. The sequences with restored *BcgI* restriction site are considered HRR products. HRR products obtained from parental cells were repaired faithfully (no mutations found), whereas the products from BCR/ABL-positive cells contained mutations (overall mutation rate:  $7 \times 10^{-4}$ ) (Figure 4, Mutation frequency). Analysis of the mutations revealed that 70% of mutations involved T:A → C:G transitions and mutation of T was detected in 50% cases (Figure 4, Mutation phenotype). These mutations do not cluster near the DSB site (Figure 4, Mutation distribution).

## DISCUSSION

We report here that BCR/ABL transformed hematopoietic cells accumulate more DSBs induced by  $\gamma$ -irradiation than parental counterparts, and that the lesions in former cells are repaired more efficiently but less faithfully. Thus, these phenomena may contribute to genomic instability associated with malignant progression of CML [4,13].

More DSBs detected in BCR/ABL cells after  $\gamma$ -irradiation may result from an additional effect of ROS induced by radiation and BCR/ABL kinase [14,27,28]. This hypothesis is supported by the observation that BCR/ABL leukemia cells contain more “spontaneous” ROS-dependent DSBs [14]. Moreover, elevated levels of DNA damage induced by etoposide, MNNG, and UVC treatment were also reported [29-31]. Although the level of DSBs in BCR/ABL transformed cells could be higher than in non-transformed counterparts, the former cells were able to repair the excess of these lesions at the same time as the latter ones implicating stimulation of DSBs repair mechanisms. These findings are contradictory to the report of Bedi and colleagues that demonstrated that BCR/ABL cells did not facilitate DSBs repair after  $\gamma$ -irradiation [32]. This discrepancy might reflect the fact that Bedi and colleagues irradiated the cells in 0°C followed by 37°C repair incubation, while we, and others used continuous incubation in 37°C. Since generation of DNA lesions and activation of DNA repair pathways usually depend on modulation of the repair pathways (which occur in 37°C rather than in 0°C) we believe that our results reflect the kinetics of DSBs repair in human body.

NHEJ and HRR appear to be more active in BCR/ABL-transformed cells in comparison to normal counterparts in accordance with previous reports [15,16]. Time-dependent engagements of NHEJ and HRR mechanisms in repair of DSBs after  $\gamma$ -irradiation are accompanied by accumulation of Ku70 and RAD51 proteins in cell lysates obtained from BCR/ABL cells in comparison to parental cells. Elevation of Ku70/80 and RAD51 after DNA damage was reported before [33,34]. Although these proteins are susceptible to caspase 3 and proteasome-dependent degradation [35-37], experiments with the use of Z-VAD-FMK and epoxomicin revealed that caspase 3 and proteasomes did not contribute to the low levels of Ku70/80 and RAD51 in parental cells (data not shown). Therefore, other mechanisms seem responsible for accumulation of these proteins in  $\gamma$ -irradiated leukemia

cells. It has been reported that BCR/ABL induces downmodulation of DNA-PKcs [38], one of the key proteins in NHEJ, suggesting that NHEJ does not play an important role in DSB repair in CML. Conversely, we detected similar expression levels of DNA-PKcs protein in normal and BCR/ABL cells before and after irradiation (data not shown). The reason for this discrepancy is not known; it may depend on different cell lysis protocol, which in our case includes DNase digestion to release the proteins associated with DNA into a soluble fraction of cell lysate.

Immunofluorescent co-localization studies revealed time-dependent increase of the number of total cellular NHEJ and HRR events 10-30min. and 3h after  $\gamma$ -irradiation, respectively, in BCR/ABL cells in comparison to parental counterparts. However, while the increase of the number of total cellular NHEJ events in BCR/ABL cells may depend on the elevated levels of DSBs, the increase of the frequency of HRR events appear to be dependent on qualitative changes in DSBs repair. The latter statement is based on the observation that the frequency of  $\gamma$ -H2AX foci co-localizing with RAD51, which implicate the assembly of HRR elements on a DSB [22], is significantly higher in BCR/ABL cells in comparison to normal counterparts. This effect might depend on BCR/ABL kinase-mediated modification of HRR machinery, for example RAD51 Y315 phosphorylation [16] which accelerates nuclear localization of RAD51 (data not shown).

Detection of  $\gamma$ -H2AX + Ku70 and  $\gamma$ -H2AX + RAD51 foci implicates the assembly of repair proteins, but it does not ultimately indicate that DSBs are actually repaired by NHEJ and HRR, respectively. Specific DSBs repair assays confirmed that BCR/ABL leukemia cells in comparison to normal cells displayed enhanced capability of HRR and NHEJ. However, DSBs repair was less faithful in former cells generating large deletions and point mutations in NHEJ and HRR products, respectively. Low fidelity of DSBs repair, including large deletions and point mutations, was reported before by our group using non-hematopoietic cells transformed by BCR/ABL [14].

Interestingly, the phenotype of point mutations identified here in HRR products in BCR/ABL leukemia cells (A $\rightarrow$ G and T $\rightarrow$ C) is different from that previously described in BCR/ABL-transformed non-hematopoietic cells [14]. AT mutator phenotype suggests the involvement of error-prone DNA polymerases during HRR, such as pol  $\eta$ , which preferentially makes errors when copying A and T template nucleotides [39]. On the other hand, a high frequency of T $\rightarrow$ C substitutions implicated pol  $\iota$ , which has the unprecedented characteristic of preferring to insert G instead of A opposite a template T [40]. The involvement of these error-prone polymerases and also pol  $\zeta$  in recombinational repair has been shown previously [41-43]. In addition, we cannot exclude the mutagenic role of pol  $\beta$ , which expression is elevated in BCR/ABL cells [9], and may eventually replace other polymerases usually involved in DNA replication during HRR [44].

Mutations in the HRR products from BCR/ABL cells do not cluster near the DSB site, but are on average about 340 bp from the site. Interestingly, conversion tracts described before in embryonic stem cells for *neo* reporter averaged only about 60 bp [45] with 80% of the recombinant having tracts of 58 bp or less [46], while 230 bp long tracts were reported in Chinese hamster ovary cells [47]. Therefore, this suggests that BCR/ABL cells display more extensive gene conversion, which increases the chance of genetic aberrations. Longer gene conversions were observed in cells lacking XRCC3 [47]. Since BCR/ABL might downregulate XRCC3 [16], this could contribute to longer gene conversions.

The molecular explanation for more extensive degradation of DSBs preceding NHEJ in cell lysates from BCR/ABL cells is unknown. Although the presence of Ku proteins is usually associated with stabilization of broken DSB ends [48], the aberrant regulation of

exonucleases such as WRN may be responsible for more extensive DSBs end-processing. BCR/ABL stimulates the expression of WRN [49], which exonuclease activity is greatly enhanced upon interaction with Ku proteins [50]. In addition, 20% of NHEJ products generated by BCR/ABL cell lysates from blunt-ended DSBs lose more than 100 bp. A similar observation was described in aggressive human bladder carcinoma, which was associated with functional Mre11/Rad50/Nbs1 complex but not with Ku70, DNA-PKcs and XRCC4 [51]. Mre11 and Nbs1 are stimulated in BCR/ABL cells (data not shown) and may eventually contribute to such phenomenon. However, a significant surplus of  $\gamma$ -H2AX foci co-localizing with Ku70 and RAD51 (especially at 3h after irradiation) suggests that some DSBs may be initially processed by HRR mechanisms and finished by NHEJ. For example, sporadic degradation of the single-stranded 3' DNA tails, which initiate HRR [52], may arrest recombination at early stage and allow the switch to NHEJ, thus generating larger deletions.

In summary, BCR/ABL leukemia cells display facilitated, but unfaithful HRR and NHEJ, which may contribute to accumulation of generic errors leading to malignant disease progression.

## Acknowledgments

This work was sponsored by the grants from National Institutes of Health and American Cancer Society (T.Skorski). A.Slupianek was sponsored by the Leukemia Research Foundation. T.Skorski was a Scholar of the Leukemia and Lymphoma Society.

## REFERENCES

- [1]. Epner DE, Koeffler HP. Molecular genetic advances in chronic myelogenous leukemia. *Ann Intern Med* 1990;113:3–6. see comments. [PubMed: 2073245]
- [2]. Clark SS, McLaughlin J, Timmons M, Pendergast AM, Ben-Neriah Y, Dow LW, Crist W, Rovera G, Smith SD, Witte ON. Expression of a distinctive BCR-ABL oncogene in Ph1-positive acute lymphocytic leukemia (ALL). *Science* 1988;239:775–777. [PubMed: 3422516]
- [3]. Sawyers CL. Signal transduction pathways involved in BCR-ABL transformation. *Baillieres Clin Haematol* 1997;10:223–231. [PubMed: 9376661]
- [4]. Skorski T. BCR/ABL regulates response to DNA damage: the role in resistance to genotoxic treatment and in genomic instability. *Oncogene* 2002;21:8591–8604. [PubMed: 12476306]
- [5]. Slupianek A, Hoser G, Majsterek I, Bronisz A, Malecki M, Blasiak J, Fishel R, Skorski T. Fusion tyrosine kinases induce drug resistance by stimulation of homology-dependent recombination repair, prolongation of G(2)/M phase, and protection from apoptosis. *Mol Cell Biol* 2002;22:4189–4201. [PubMed: 12024032]
- [6]. Shet AS, Jahagirdar BN, Verfaillie CM. Chronic myelogenous leukemia: mechanisms underlying disease progression. *Leukemia* 2002;16:1402–1411. [PubMed: 12145676]
- [7]. Ilaria R Jr. Bcr/Abl, leukemogenesis, and genomic instability: a complex partnership. *Leuk Res* 2002;26:971–973. [PubMed: 12363461]
- [8]. Salloukh HF, Laneuville P. Increase in mutant frequencies in mice expressing the BCR-ABL activated tyrosine kinase. *Leukemia* 2000;14:1401–1404. [PubMed: 10942235]
- [9]. Canitrot Y, Lautier D, Laurent G, Frechet M, Ahmed A, Turhan AG, Salles B, Cazaux C, Hoffmann JS. Mutator phenotype of BCR--ABL transfected Ba/F3 cell lines and its association with enhanced expression of DNA polymerase beta. *Oncogene* 1999;18:2676–2680. [PubMed: 10348341]
- [10]. Klucher KM, Lopez DV, Daley GQ. Secondary mutation maintains the transformed state in BaF3 cells with inducible BCR/ABL expression. *Blood* 1998;91:3927–3934. [PubMed: 9573031]
- [11]. Deutsch E, Jarrousse S, Buet D, Dugray A, Bonnet ML, Vozenin-Brotons MC, Guilhot F, Turhan AG, Feunteun J, Bourhis J. Down-regulation of BRCA1 in BCR-ABL-expressing hematopoietic cells. *Blood* 2003;101:4583–4588. [PubMed: 12576338]

- [12]. Canitrot Y, Falinski R, Louat T, Laurent G, Cazaux C, Hoffmann JS, Lautier D, Skorski T. p210 BCR/ABL kinase regulates nucleotide excision repair (NER) and resistance to UV radiation. *Blood* 2003;102:2632–2637. [PubMed: 12829601]
- [13]. Calabretta B, Perrotti D. The biology of CML blast crisis. *Blood* 2004;103:4010–4022. [PubMed: 14982876]
- [14]. Nowicki MO, Falinski R, Koptyra M, Slupianek A, Stoklosa T, Gloc E, Nieborowska-Skorska M, Blasiak J, Skorski T. BCR/ABL oncogenic kinase promotes unfaithful repair of the reactive oxygen species-dependent DNA double-strand breaks. *Blood* 2004;104:3746–3753. [PubMed: 15304390]
- [15]. Gaymes TJ, Mufti GJ, Rassool FV. Myeloid leukemias have increased activity of the nonhomologous end-joining pathway and concomitant DNA misrepair that is dependent on the Ku70/86 heterodimer. *Cancer Res* 2002;62:2791–2797. [PubMed: 12019155]
- [16]. Slupianek A, Schmutte C, Tomblin G, Nieborowska-Skorska M, Hoser G, Nowicki MO, Pierce AJ, Fishel R, Skorski T. BCR/ABL regulates mammalian RecA homologs, resulting in drug resistance. *Mol Cell* 2001;8:795–806. [PubMed: 11684015]
- [17]. Pierce AJ, Johnson RD, Thompson LH, Jasin M. XRCC3 promotes homology-directed repair of DNA damage in mammalian cells. *Genes Dev* 1999;13:2633–2638. [PubMed: 10541549]
- [18]. Trojanek J, Ho T, Del Valle L, Nowicki M, Wang JY, Lassak A, Peruzzi F, Khalili K, Skorski T, Reiss K. Role of the insulin-like growth factor I/insulin receptor substrate 1 axis in Rad51 trafficking and DNA repair by homologous recombination. *Mol Cell Biol* 2003;23:7510–7524. [PubMed: 14559999]
- [19]. Burma S, Chen BP, Murphy M, Kurimasa A, Chen DJ. ATM phosphorylates histone H2AX in response to DNA double-strand breaks. *J Biol Chem* 2001;276:42462–42467. [PubMed: 11571274]
- [20]. Rogakou EP, Boon C, Redon C, Bonner WM. Megabase chromatin domains involved in DNA double-strand breaks in vivo. *J Cell Biol* 1999;146:905–916. [PubMed: 10477747]
- [21]. Ward IM, Chen J. Histone H2AX is phosphorylated in an ATR-dependent manner in response to replicational stress. *J Biol Chem* 2001;276:47759–47762. [PubMed: 11673449]
- [22]. Paull TT, Rogakou EP, Yamazaki V, Kirchgessner CU, Gellert M, Bonner WM. A critical role for histone H2AX in recruitment of repair factors to nuclear foci after DNA damage. *Curr Biol* 2000;10:886–895. [PubMed: 10959836]
- [23]. Rapp A, Greulich KO. After double-strand break induction by UV-A, homologous recombination and nonhomologous end joining cooperate at the same DSB if both systems are available. *J Cell Sci* 2004;117:4935–4945. [PubMed: 15367581]
- [24]. Wang H, Zeng ZC, Bui TA, Sonoda E, Takata M, Takeda S, Iliakis G. Efficient rejoining of radiation-induced DNA double-strand breaks in vertebrate cells deficient in genes of the RAD52 epistasis group. *Oncogene* 2001;20:2212–2224. [PubMed: 11402316]
- [25]. Baumann P, West SC. DNA end-joining catalyzed by human cell-free extracts. *Proc Natl Acad Sci U S A* 1998;95:14066–14070. [PubMed: 9826654]
- [26]. Labhart P. Nonhomologous DNA end joining in cell-free systems. *Eur J Biochem* 1999;265:849–861. [PubMed: 10518778]
- [27]. Sattler M, Verma S, Shrikhande G, Byrne CH, Pride YB, Winkler T, Greenfield EA, Salgia R, Griffin JD. The BCR/ABL tyrosine kinase induces production of reactive oxygen species in hematopoietic cells. *J Biol Chem* 2000;275:24273–24278. [PubMed: 10833515]
- [28]. Kovacic P, Jacintho JD. Reproductive toxins: pervasive theme of oxidative stress and electron transfer. *Curr Med Chem* 2001;8:863–892. [PubMed: 11375756]
- [29]. Hoser G, Majsterek I, Romana DL, Slupianek A, Blasiak J, Skorski T. Fusion oncogenic tyrosine kinases alter DNA damage and repair after genotoxic treatment: role in drug resistance? *Leuk Res* 2003;27:267–273. [PubMed: 12537980]
- [30]. Dierov J, Dierova R, Carroll M. BCR/ABL translocates to the nucleus and disrupts an ATR-dependent intra-S phase checkpoint. *Cancer Cell* 2004;5:275–285. [PubMed: 15050919]
- [31]. Laurent E, Mitchell DL, Estrov Z, Lowery M, Tucker SL, Talpaz M, Kurzrock R. Impact of p210(Bcr-Abl) on ultraviolet C wavelength-induced DNA damage and repair. *Clin Cancer Res* 2003;9:3722–3730. [PubMed: 14506164]



- [32]. Bedi A, Barber JP, Bedi GC, el-Deiry WS, Sidransky D, Vala MS, Akhtar AJ, Hilton J, Jones RJ. BCR-ABL-mediated inhibition of apoptosis with delay of G2/M transition after DNA damage: a mechanism of resistance to multiple anticancer agents. *Blood* 1995;86:1148–1158. [PubMed: 7620167]
- [33]. Christodouloupoulos G, Malapetsa A, Schipper H, Golub E, Radding C, Panasci LC. Chlorambucil induction of HsRad51 in B-cell chronic lymphocytic leukemia. *Clin Cancer Res* 1999;5:2178–2184. [PubMed: 10473103]
- [34]. Kumaravel TS, Bharathy K, Kudoh S, Tanaka K, Kamada N. Expression, localization and functional interactions of Ku70 subunit of DNA-PK in peripheral lymphocytes and Nalm-19 cells after irradiation. *Int J Radiat Biol* 1998;74:481–489. [PubMed: 9798959]
- [35]. Huang Y, Nakada S, Ishiko T, Utsugisawa T, Datta R, Kharbanda S, Yoshida K, Talanian RV, Weichselbaum R, Kufe D, Yuan Z-M. Role for Caspase-Mediated Cleavage of Rad51 in Induction of Apoptosis by DNA Damage. *Mol Cell Biol* 1999;19:2986–2997. [PubMed: 10082566]
- [36]. Kim SH, Kim D, Han JS, Jeong CS, Chung BS, Kang CD, Li GC. Ku autoantigen affects the susceptibility to anticancer drugs. *Cancer Res* 1999;59:4012–4017. [PubMed: 10463600]
- [37]. Wang JY, Ho T, Trojanek J, Chintapalli J, Grabacka M, Stoklosa T, Garcia FU, Skorski T, Reiss K. Impaired homologous recombination DNA repair and enhanced sensitivity to DNA damage in prostate cancer cells exposed to anchorage-independence. *Oncogene* 2005;24:3748–3758. [PubMed: 15782124]
- [38]. Deutsch E, Dugray A, AbdulKarim B, Marangoni E, Maggiorella L, Vaganay S, M'Kacher R, Rasy SD, Eschwege F, Vainchenker W, Turhan AG, Bourhis J. BCR-ABL down-regulates the DNA repair protein DNA-PKcs. *Blood* 2001;97:2084–2090. [PubMed: 11264175]
- [39]. Matsuda T, Bebenek K, Masutani C, Hanaoka F, Kunkel TA. Low fidelity DNA synthesis by human DNA polymerase-eta. *Nature* 2000;404:1011–1013. [PubMed: 10801132]
- [40]. Zhang Y, Yuan F, Wu X, Wang Z. Preferential incorporation of G opposite template T by the low-fidelity human DNA polymerase iota. *Mol Cell Biol* 2000;20:7099–7108. [PubMed: 10982826]
- [41]. Holbeck SL, Strathern JN. A role for REV3 in mutagenesis during double-strand break repair in *Saccharomyces cerevisiae*. *Genetics* 1997;147:1017–1024. [PubMed: 9383049]
- [42]. Kannouche P, Broughton BC, Volker M, Hanaoka F, Mullenders LH, Lehmann AR. Domain structure, localization, and function of DNA polymerase eta, defective in xeroderma pigmentosum variant cells. *Genes Dev* 2001;15:158–172. [PubMed: 11157773]
- [43]. Kannouche P, Fernandez De Henestrosa AR, Coull B, Vidal AE, Gray C, Zicha D, Woodgate R, Lehmann AR. Localization of DNA polymerases eta and iota to the replication machinery is tightly co-ordinated in human cells. *Embo J* 2002;21:6246–6256. [PubMed: 12426396]
- [44]. Servant L, Bieth A, Hayakawa H, Cazaux C, Hoffmann JS. Involvement of DNA polymerase beta in DNA replication and mutagenic consequences. *J Mol Biol* 2002;315:1039–1047. [PubMed: 11827474]
- [45]. Stark JM, Pierce AJ, Oh J, Pastink A, Jasin M. Genetic steps of mammalian homologous repair with distinct mutagenic consequences. *Mol Cell Biol* 2004;24:9305–9316. [PubMed: 15485900]
- [46]. Elliott B, Richardson C, Winderbaum J, Nickoloff JA, Jasin M. Gene conversion tracts from double-strand break repair in mammalian cells. *Mol Cell Biol* 1998;18:93–101. [PubMed: 9418857]
- [47]. Brenneman MA, Wagener BM, Miller CA, Allen C, Nickoloff JA. XRCC3 controls the fidelity of homologous recombination: roles for XRCC3 in late stages of recombination. *Mol Cell* 2002;10:387–395. [PubMed: 12191483]
- [48]. Featherstone C, Jackson SP. Ku, a DNA repair protein with multiple cellular functions? *Mutat Res* 1999;434:3–15. [PubMed: 10377944]
- [49]. Slupianek A, Gurdek E, Koptyra M, Nowicki MO, Siddiqui KM, Groden J, Skorski T. BLM helicase is activated in BCR/ABL leukemia cells to modulate responses to cisplatin. *Oncogene* 2005;24:3914–3922. [PubMed: 15750625]

- [50]. Orren DK, Machwe A, Karmakar P, Piotrowski J, Cooper MP, Bohr VA. A functional interaction of Ku with Werner exonuclease facilitates digestion of damaged DNA. *Nucleic Acids Res* 2001;29:1926–1934. [PubMed: 11328876]
- [51]. Bentley J, Diggle CP, Harnden P, Knowles MA, Kiltie AE. DNA double strand break repair in human bladder cancer is error prone and involves microhomology-associated end-joining. *Nucleic Acids Res* 2004;32:5249–5259. [PubMed: 15466592]
- [52]. Szostak JW, Orr-Weaver TL, Rothstein RJ, Stahl FW. The double-strand-break repair model for recombination. *Cell* 1983;33:25–35. [PubMed: 6380756]

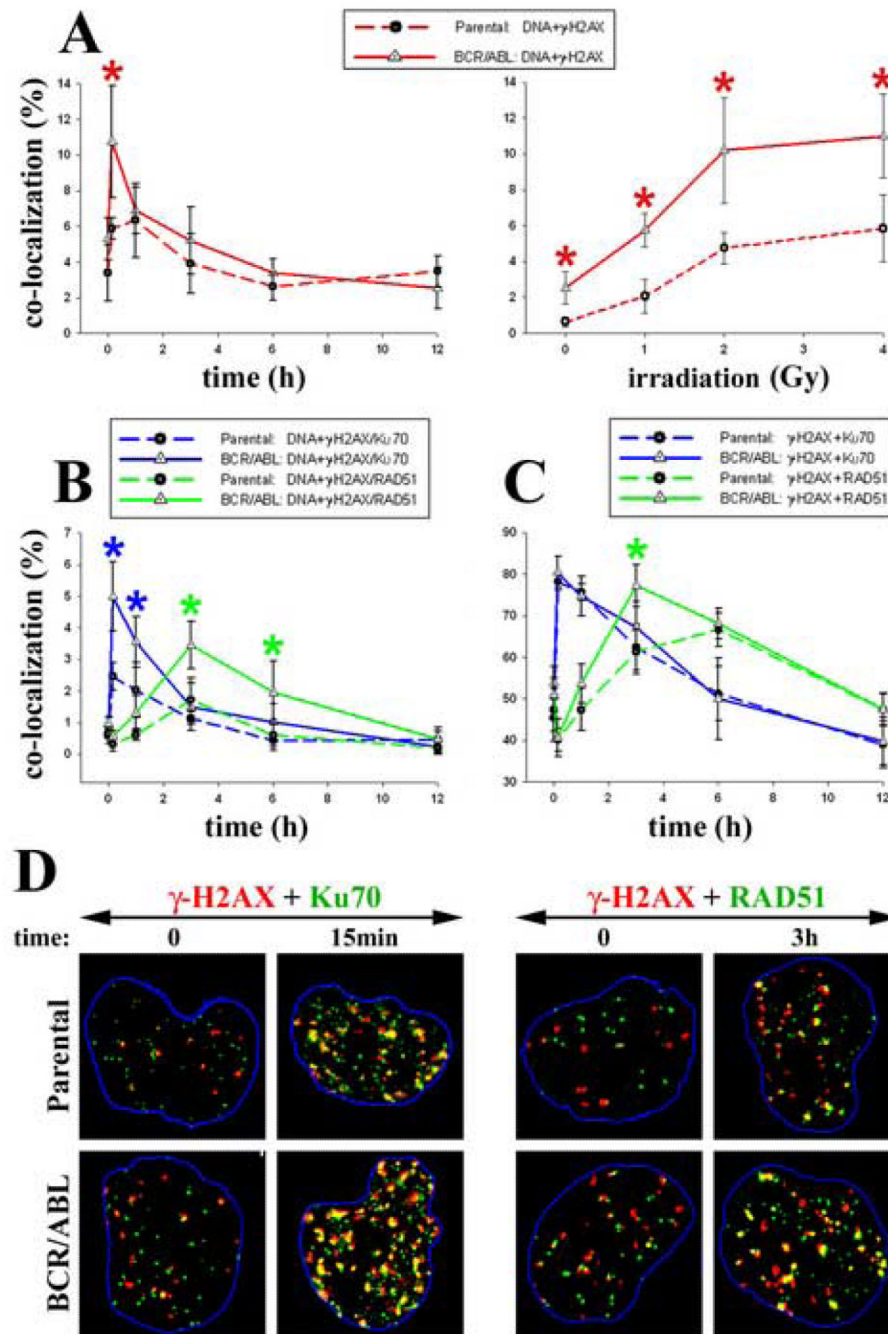


**Figure 1. BCR/ABL modified the kinetics of DSBs accumulation and repair**  
 32Dcl3 (Parental) and BCR/ABL-32Dcl3 (BCR/ABL) cells were irradiated with 4Gy (**A-left panel, B-D**) or with the indicated doses (**A-right panel**) and the nuclear foci were detected: (**A**)  $\gamma$ -H2AX foci co-localized with DNA counterstained with DAPI; (**B**) double-stained  $\gamma$ -H2AX + RAD51 foci or  $\gamma$ -H2AX + KU70 foci co-localized with DNA; and (**C**) KU70 or RAD51 foci co-localized with  $\gamma$ -H2AX foci. (\* $p < 0.01$ , in comparison to Parental group). (**D**) Representative nuclear staining for  $\gamma$ -H2AX and Ku70 or  $\gamma$ -H2AX and RAD51 foci at the indicated time after irradiation with 4Gy; yellow foci represent co-localization. Nuclei borders are marked in blue.

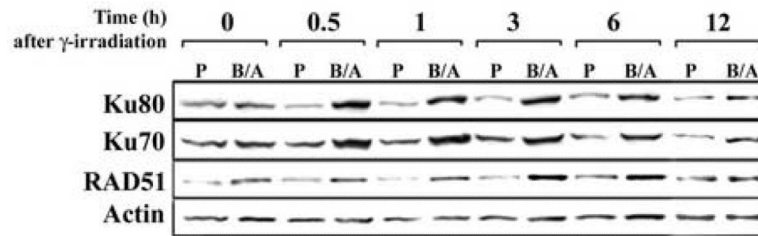


**Figure 2. BCR/ABL affects the expression of DSBs repair protein after  $\gamma$ -irradiation**

Expression of the proteins directly responsible for NHEJ (Ku70, Ku80) and HRR (RAD51) was examined at various times after 4Gy of  $\gamma$ -irradiation in 32Dcl3 parental (P) and BCR/ABL-positive counterparts (B/A). Lysis buffer containing DNase was used to release the DNA-bound proteins to the cell lysate. Actin served as a loading control.

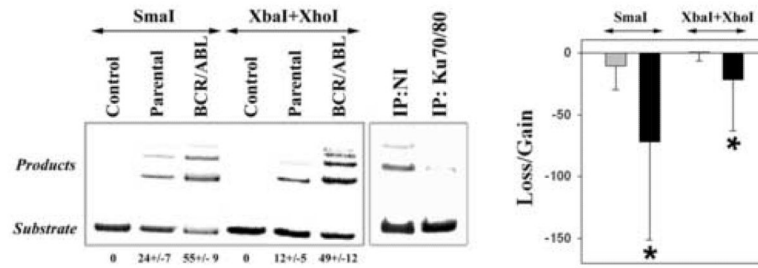


**Figure 3. BCR/ABL promotes unfaithful NHEJ**

NHEJ-mediated end-ligation of the SmaI or XhoI+XbaI – digested plasmid substrate (monomers) by the lysis buffer (Control), or cell lysates from 32Dcl3 (Parental), and BCR/ABL-32Dcl3 (BCR/ABL) cells, generating multi-plasmid products (dimers, trimers). The mean percentages of end-joined substrate  $\pm$  SD are shown below ( $p < 0.01$ , BCR/ABL in comparison to Parental). The reaction was abrogated after deprivation of cell lysate from Ku70 and Ku80. The average  $\pm$  SD gain/loss of DNA bases per individual reaction is shown;  $*p < 0.05$ .

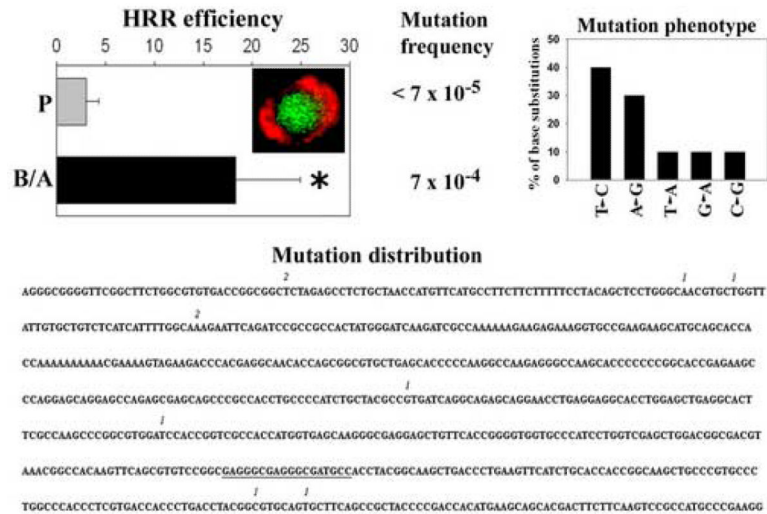


**Figure 4. BCR/ABL promotes unfaithful HRR in leukemia cells**

32Dcl3-DR-GFP parental cells (P) and BCR/ABL-positive counterparts (B/A) containing a single copy of the DR-GFP recombination cassette integrated in their genome were transfected with I-SceI and pDsRed1-Mito expression plasmids. Expression of I-SceI may cause a DSB in the specific restriction site included in the DR-GFP cassette, and pDsRed1-Mito encodes red fluorescent protein to control the efficiency of transfection. HRR event restores functional GFP expression, which is readily detected by fluorescent microscope 48h after transfection with I-SceI. HRR efficiency is shown as % of cells with both green nuclear fluorescence and red mitochondrial fluorescence (see inset) versus all transfected (red) cells. Results represent mean  $\pm$  SD from 3 clones in each group; \* $p < 0.01$ . Mutation frequency, Mutation phenotype and Mutation distribution (numbers indicate the number of mutations detected at the particular base) in HRR products obtained from BCR/ABL-positive cells are shown. Location of the former I-SceI site is underlined.